INTERNATIONAL JOURNAL OF ADAPTIVE CONTROL AND SIGNAL PROCESSING
Int. J. Adapt. Control Signal Process. 2008; **22**:374–387
Published online 8 August 2007 in Wiley InterScience (www.interscience.wiley.com). DOI: 10.1002/acs.990

H_∞ compensation of external vibration impact on servo performance of hard disk drives in mobile applications

C. Du[1,*,†], S. S. Ge[2] and F. L. Lewis[3]

[1]*A*STAR, Data Storage Institute (DSI), 5 Engineering Drive 1, Singapore 117608, Singapore*
[2]*Department of Electrical and Computer Engineering, National University of Singapore, Singapore 117576, Singapore*
[3]*Automation and Robotics Research Institute, University of Texas, Arlington, TX 76019, U.S.A.*

SUMMARY

H_∞ compensation for external vibration impact on the positioning accuracy of hard disk drives is considered in this paper. A feedforward controller is designed to attenuate the impact with the aid of a sensor to detect external vibrations. Loop shaping in frequency domain and H_∞ method in state space are used to design the feedforward controller. The linear matrix inequality approach is adopted for solving the H_∞ feedforward control design problem. The application results in a 1.8-in disk drive with an accelerometer to measure acceleration signal show that 97% reduction of the position error signal is achieved with the feedforward control designed by the H_∞ method. The effectiveness of the two methods is also evaluated and compared when external vibration model is subjected to gain variations. Copyright © 2007 John Wiley & Sons, Ltd.

Received 24 October 2006; Revised 2 May 2007; Accepted 20 June 2007

KEY WORDS: acceleration feedforward; external vibration compensation; hard disk drives; H_∞ control; linear matrix inequality; servo control

1. INTRODUCTION

As the demand for big capacity hard disk drives (HDDs) achieved mainly through enhancing recording density is growing continuously [1], more stringent requirement on the positioning

*Correspondence to: C. Du, A*STAR, Data Storage Institute (DSI), 5 Engineering Drive 1, Singapore 117608, Singapore.
†E-mail: du_chunling@dsi.a-star.edu.sg

Contract/grant sponsor: Publishing Arts Research Council; contract/grant number: 98-1846389
Contract/grant sponsor: A*Star SERC; contract/grant number: 052 101 0097

accuracy within a narrower track width [2] is thus created along with the advancement in head and media. Consequently, the importance of the ability to accurately position the read/write (R/W) head through the voice-coil-motor (VCM) actuator becomes more critical. A great deal of attention has been paid to the improvement of positioning accuracy *via* servo control performance enhancement [3–5].

In recent years, the trend toward smaller form factor is prosperous in the magnetic disk storage industry, as HDDs enter mobile applications such as portable music players, portable photo/video viewers, and automotive systems [6]. Small disk drives are designed for operating in extreme environment or consumer electronics products and thus need to resist much more severe external shocks and vibrations [7] than conventional disk drives such as those used in desktop computers. These external disturbances deteriorate positioning accuracy of the R/W head on the desired track, and consequently impair data flow smoothness during reading and writing, or even spoil data recorded on the disk.

External vibrations dominate at relatively low frequencies [8, 9], and thus to reject the external vibration a servo control with a high gain in the low-frequency range is desired. However, it will diminish the rejection capability to higher-frequency vibrations due to Bode water-bed effect [10]. As suggested by many authors [11, 12], accelerometers are used to detect acceleration signal for external vibration rejection. Feedforward control schemes are then proposed with the acceleration signal injected as an input, in order to reduce bad influence of external vibrations on positioning accuracy of R/W head. Due to low cost, small size and high quality as sensor technology advances, it is feasible to include accelerometers in a product disk drive. We know shock sensors are already used in some of current disk drive products for detecting external shock vibrations so as to prevent malfunctioning of writing and reading in case of severe shock. There are many papers dedicated to the acceleration feedforward scheme in order to improve the track-following performance. An adaptive feedforward controller with FIR filter form is designed in [9] using dynamics between the accelerometer and the position error signal (PES). In [13], correction of accelerometer phase delay in feedforward control design is considered. A disturbance observer is utilized to estimate disturbances in [14], where the dynamics between the accelerometer and the disturbance is used for feedforward control design. In [15], a feedforward control scheme is employed effectively for disk fluttering induced vibration compensation by using optical sensors to detect disk vibration.

In this paper, the problem of external vibration compensation for improving actuator positioning accuracy in disk drives is formulated. With a detection sensor for external vibrations, loop shaping in frequency domain and H_∞ method in state space are proposed for designing the feedforward controller. The feedforward controller design is carried out for a 1.8-in small disk drive with an accelerometer for measuring the acceleration signal due to the external vibrations. Application results are presented to show the effectiveness of the designed feedforward controllers in the compensation for external vibration impact on positioning accuracy. Additionally, the performance of the designed feedforward controllers is evaluated for varying vibration models. It turns out that the H_∞ controller is more robust than that of loop shaping. The main contributions of this paper are as follows: (1) The compensation problem of external vibration impact on positioning accuracy is formulated as an H_∞ feedforward control problem. (2) The H_∞ feedforward controller is designed with an LMI approach. (3) It results in a remarkable attenuation to the impact of external vibrations.

DOI: 10.1002/acs

2. SYSTEM DESCRIPTION AND PROBLEM STATEMENT FOR EXTERNAL VIBRATION COMPENSATION

The disk drive under consideration is a Hitachi GST 1.8-in HDD as shown in Figure 1 with model number HTC426020G7AT00 and spindle motor rotational speed 4200 RPM. The servo loop of disk drives is shown in Figure 2, where $P(s)$ is the VCM positioner model, $C(z)$ is the feedback controller. Figure 3 shows the frequency response of VCM positioner of the 1.8-in disk drive.

Figure 1. Hitachi GST 1.8-in disk dive.

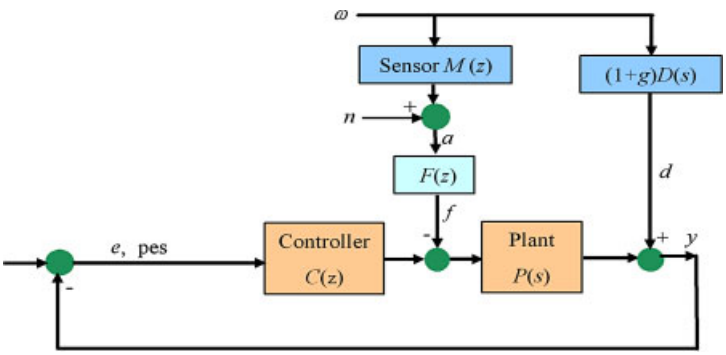

Figure 2. Control system for external vibration compensation.

DOI: 10.1002/acs

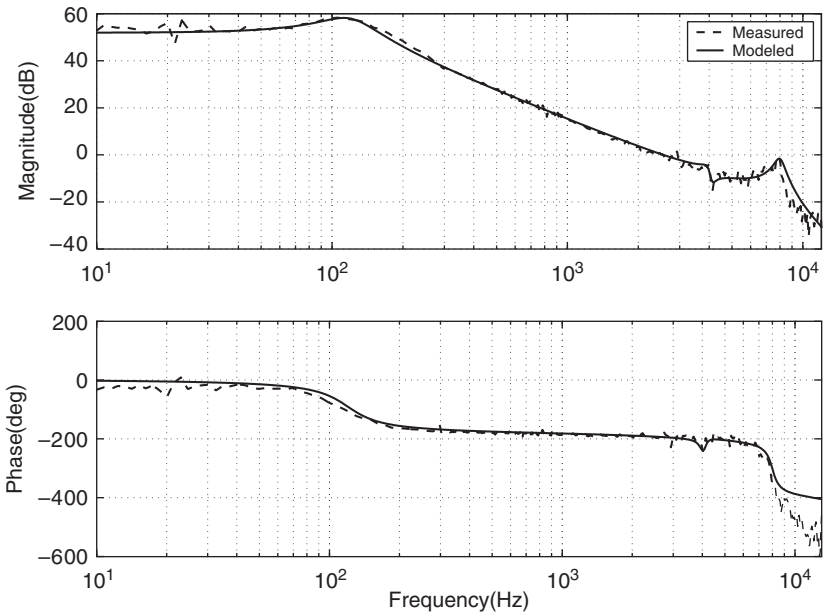

Figure 3. Frequency response of the VCM actuator.

The model $P(s)$ described by

$$\text{zeros} = 10^5 \times [1.6965;\ -0.0077 \pm 0.2575i]$$

$$\text{poles} = 10^5 \times [-1.6965;\ -0.0251 \pm 0.5020i;\ -0.0101 \pm 0.2511i;\ -0.0019 \pm 0.0073i]$$

$$\text{gain} = -5.3167 \times 10^{17}$$

is obtained by curve fitting to the measured frequency response in Figure 3. The feedback controller $C(z)$ with a sampling rate of 30 kHz is given in (1), which is a typical PID (proportional-integral-derivative) controller combined with two notch filters at 4.2 and 8 kHz, as shown in Figure 4. The open-loop bandwidth is 1.4 kHz, the gain margin and phase margin are 7.7 dB and 50°, respectively:

$$C(z) = \frac{0.6634(z^2 - 1.936z + 0.9375)(z^2 - 1.222z + 0.9158)(z^2 + 0.1627z + 0.7153)}{z(z-1)(z^2 - 0.1034z + 0.1872)(z^2 - 1.174z + 0.8387)} \tag{1}$$

In Figure 2, e or *pes* is the position error signal, $M(z)$ represents the model of the sensor to detect external vibrations, n is the sensing noise, w is external vibrations acting on the actuator, $D(s)$ is the transfer function from the external vibrations to the actuator, and g represents the gain variation of $D(s)$. Figure 5 shows the change of position error spectrum when the system is subjected to external vibrations, and the impact of the external vibrations on the positioning accuracy is severe especially in lower frequencies than 800 Hz.

The external vibration compensation problem is stated as follows: *design a stable feedforward controller $F(z)$ such that the standard deviation (or σ value) of error e due to the external vibration w is minimized.*

DOI: 10.1002/acs

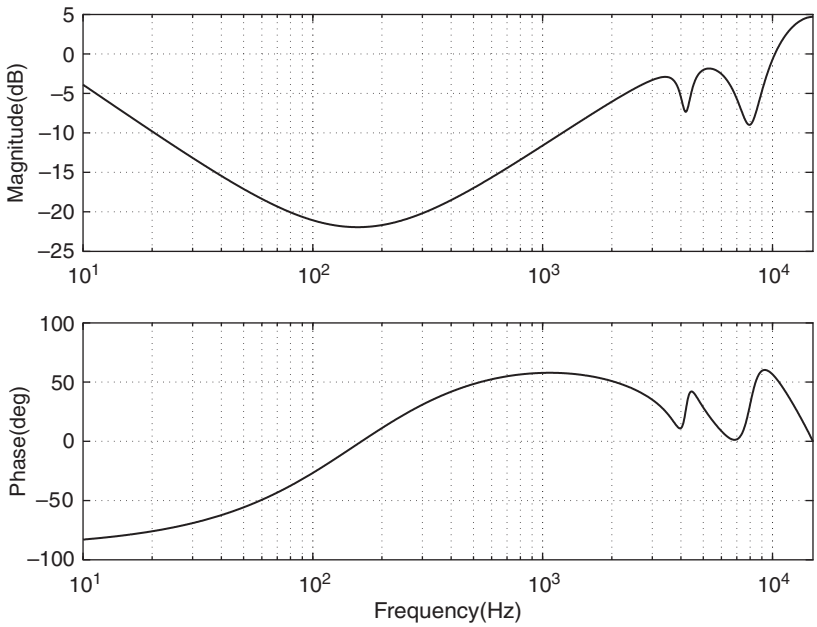

Figure 4. Frequency response of controller $C(z)$.

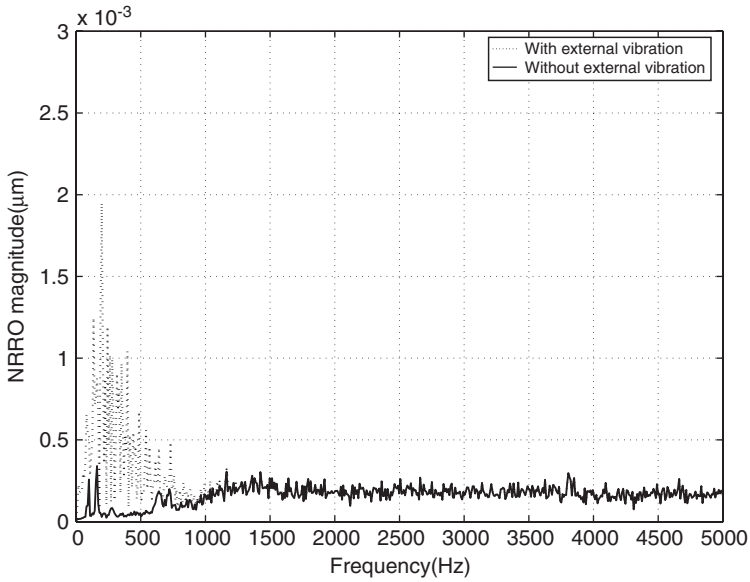

Figure 5. Position error spectrum with and without external vibrations.

DOI: 10.1002/acs

In the next section, two methods, namely loop shaping and H_∞ methods, are introduced and we focus on how to use the two methods to design the feedforward controller $F(z)$ such that the above purpose is fulfilled.

3. FEEDFORWARD CONTROLLER $F(z)$ DESIGN METHODS

In this section, we present how to design the feedforward controller $F(z)$ by loop shaping in frequency domain, and H_∞ method in state space. The loop shaping uses curve fitting to frequency response to obtain the transfer function of the feedforward controller, and the H_∞ method applies the linear matrix inequality (LMI) approach to parameterize the state-space model of the feedforward controller.

3.1. Loop shaping

Let $T_{ew}: w \to e$ denote the transfer function from w to e. From Figure 2, T_{ew} is given by

$$T_{ew}(z) = \frac{F(z)M(z)P(z)}{1 + C(z)P(z)} - \frac{D(z)}{1 + C(z)P(z)} \tag{2}$$

where $P(z)$ is the discrete-time model of $P(s)$ by discretizing it with zero-order-hold method, and $D(z)$ is the discrete form of $D(s)$ subjected to discretization with any appropriate method.

The ideal case is that when $D(z) = F(z)M(z)P(z)$, the error e is zero. It follows that

$$F(z) = D(z)[M(z)P(z)]^{-1} \tag{3}$$

With the models or frequency responses of $D(z)$, $M(z)$ and $P(z)$, the frequency response of $D(z)[M(z)P(z)]^{-1}$ can be calculated. $F(z)$ can then be found approximately by curve fitting to the frequency response of $D(z)[M(z)P(z)]^{-1}$. Although the loop shaping method is a straightforward method, it is time consuming and the solution may not exist due to the inverse in (3). Hence in what follows we introduce the H_∞ method in state space.

3.2. H_∞ method

Introduce the following state-space form of feedforward controller $F(z)$:

$$x_f(k+1) = A_f x_f(k) + B_f a(k) \tag{4}$$

$$f(k) = C_f x_f(k) + D_f a(k) \tag{5}$$

Denote (A_p, B_p, C_p, D_p) and (A_c, B_c, C_c, D_c) as the state-space realization of $P(z)$ and $C(z)$, (A_d, B_d, C_d, D_d), (A_a, B_a, C_a, D_a), respectively, the state-space realizations of $D(z)$ and $M(z)$.

Assume that $1 + D_c D_p$ is invertible, or the closed-loop system is well posed. Let $N = (1 + D_c D_p)^{-1}$. From Figure 2, we have

$$x(k+1) = Ax(k) + B_1 w(k) + B_2 f(k) \tag{6}$$

$$a(k) = C_1 x(k) + D_{11} w(k) + D_{12} f(k) + n(k) \tag{7}$$

$$e(k) = C_2 x(k) + D_{21} w(k) + D_{22} f(k) \tag{8}$$

DOI: 10.1002/acs

where

$$A=\begin{bmatrix} A_p - NB_pD_cC_p & NB_pC_c & -NB_pD_cC_d & 0 \\ -NB_cC_p & A_c - NB_cD_pC_c & -NB_cC_d & 0 \\ 0 & 0 & A_d & 0 \\ A_a & 0 & 0 & 0 \end{bmatrix}, \quad B_1=\begin{bmatrix} -NB_pD_cD_d \\ -NB_cD_d \\ B_d \\ B_a \end{bmatrix} \tag{9}$$

$$B_2=\begin{bmatrix} -NB_p \\ NB_cD_p \\ 0 \\ 0 \end{bmatrix}, \quad C_1=[0\ \ 0\ \ 0\ \ C_a], \quad D_{11}=D_a, \quad D_{12}=0 \tag{10}$$

$$C_2=[-NC_p\ \ -ND_pC_c\ \ -NC_d\ \ 0], \quad D_{21}=-ND_d, \quad D_{22}=ND_p \tag{11}$$

Associated with (6)–(8), our target is to design a dynamic feedforward controller $F(z)$ with the form of (4)–(5) such that H_∞ norm of T_{ew} is minimized. It is known that (A_f, B_f, C_f, D_f) in (4)–(5) can be obtained *via* existing LMI approach [16] based on the following theorem.

Theorem 3.1 (*Du and Guo* [*17*] *and de Oliveira et al.* [*18*])
All controllers of the form (A_f, B_f, C_f, D_f) such that $\|T_{ew}\|_\infty<\gamma$ holds are parameterized by the LMI $\Sigma<0$, and

$$\Sigma=\begin{bmatrix} -S & * & * & * & * & * \\ -I & -R & * & * & * & * \\ SA+VC_1 & U & -S & * & * & * \\ A+B_2D_fC_1 & AR+B_2Z & -I & -R & * & * \\ C_2+D_{22}D_cC_1 & C_2R+D_{22}Z & 0 & 0 & -I & * \\ 0 & 0 & B_1^{\mathrm{T}}S+D_{11}^{\mathrm{T}}V^{\mathrm{T}} & B_1^{\mathrm{T}}+D_{11}^{\mathrm{T}}D_f^{\mathrm{T}}B_2^{\mathrm{T}} & D_{21}^{\mathrm{T}}+D_{11}^{\mathrm{T}}D_f^{\mathrm{T}}D_{22}^{\mathrm{T}} & -\gamma^2 I \end{bmatrix}$$

where $*$ denotes an entry that can be deduced from the symmetry of the LMI, matrices Z, U, V, D_f and the symmetric matrices R and S are the variables. A feasible controller is then given by choosing Ξ and Λ nonsingular such that $\Xi\Lambda=I-SR$ and calculating

$$C_f=(Z-D_fC_1R)\Lambda^{-1}, \quad B_f=\Xi^{-1}(V-SB_2D_f) \tag{12}$$

$$A_f=\Xi^{-1}[U-S(A+B_2D_fC_1)R-SB_2C_f\Lambda-\Xi B_fC_1R]\Lambda^{-1} \tag{13}$$

Remark 3.1
The solution of the feedforward controller in the above theorem is in terms of the LMI, which can be efficiently solved by convex optimization [16]. In [18], it is proved that if there exist solutions Z, U, V, D_f, R and S for the LMI Σ, $\Xi\Lambda=I-SR$ is invertible. From $\Xi\Lambda=I-SR$, nonsingular matrices Ξ and Λ can be computed. Then, the computation of the controller parameters C_f, A_f, B_f can be carried out by solving (12) and (13).

DOI: 10.1002/acs

4. APPLICATION RESULTS

In Figure 2, an accelerometer is used for measuring the acceleration signal and thus the model $M(z)$ can be represented by $M(z) = ((z-1)/z)^2$ with a sensing noise n. The external vibration is assumed to be acting vertically to the disk surface, and dominates in low-frequency range [8, 9]. Thus the following model,

$$D(s) = \frac{3.757e-6s^3 + 0.3077s^2 + 1.381e4s + 8.374e8}{s^3 + 1885s^2 + 1.777e6s + 8.374e8} \tag{14}$$

i.e. a low-pass filter, is used to represent the transfer function from external vibration w to the actuator. The Bode plot of $D(s)$ is shown in Figure 6.

4.1. Loop shaping

With the models of $D(z)$, $M(z)$ and $P(z)$, the frequency response of $D(z)[M(z)P(z)]^{-1}$ is calculated and shown in Figure 7. The model $F(z)$ is subsequently attained *via* curve fitting to the frequency response of $D(z)[M(z)P(z)]^{-1}$. Due to the impact of external vibrations dominant in low-frequency range, for the curve fitting, we pay more attention up to 1 kHz. It is observed from Figure 7 that $F(z)$ matches $D(z)[M(z)P(z)]^{-1}$ very well before 1 kHz:

$$F(z) = \frac{-8.4724e-5(z-4.332)(z+1)(z^2-1.983z+0.9834)(z^2-1.859z+0.8819)}{(z-0.9999)^2(z-0.2308)(z^2-1.972z+0.9731)(z^2-1.903z+0.9089)} \tag{15}$$

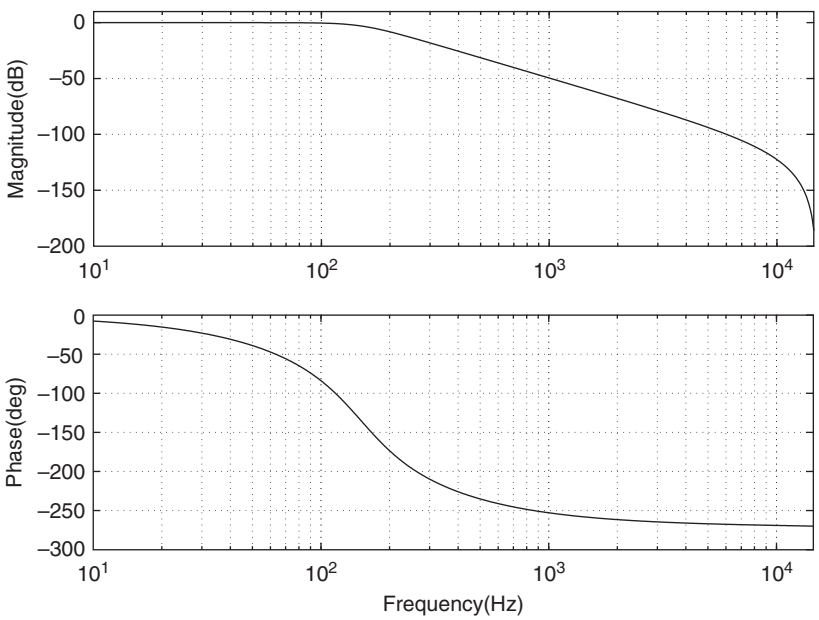

Figure 6. Frequency response of $D(s)$.

DOI: 10.1002/acs

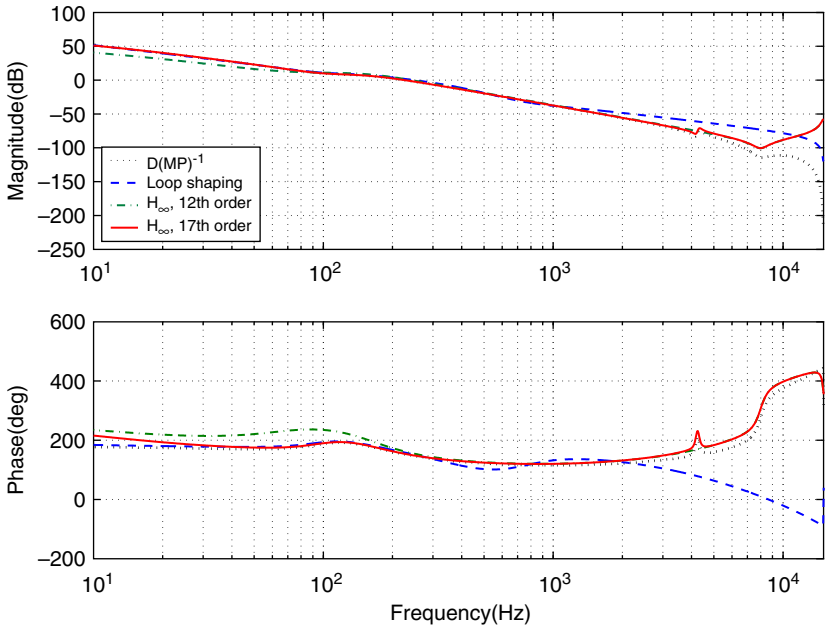

Figure 7. Frequency response of the feedforward compensator F.

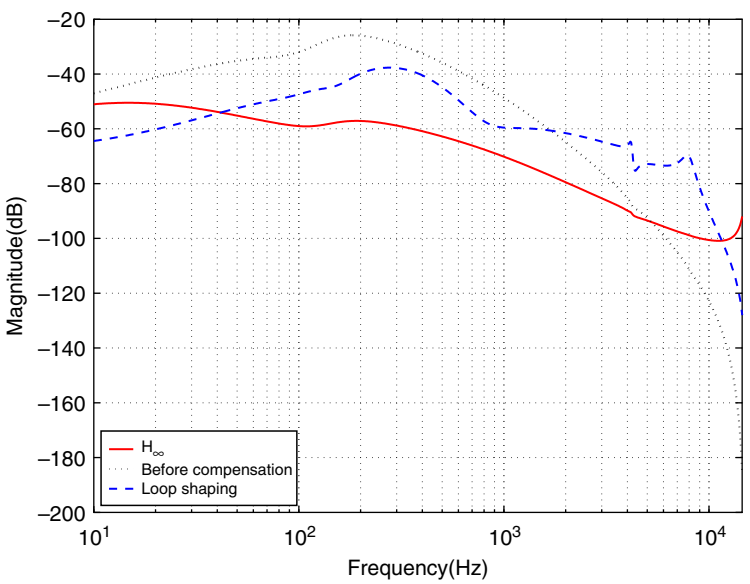

Figure 8. External vibration rejection (i.e. T_{ew}) comparison with and without the feedforward compensation.

DOI: 10.1002/acs

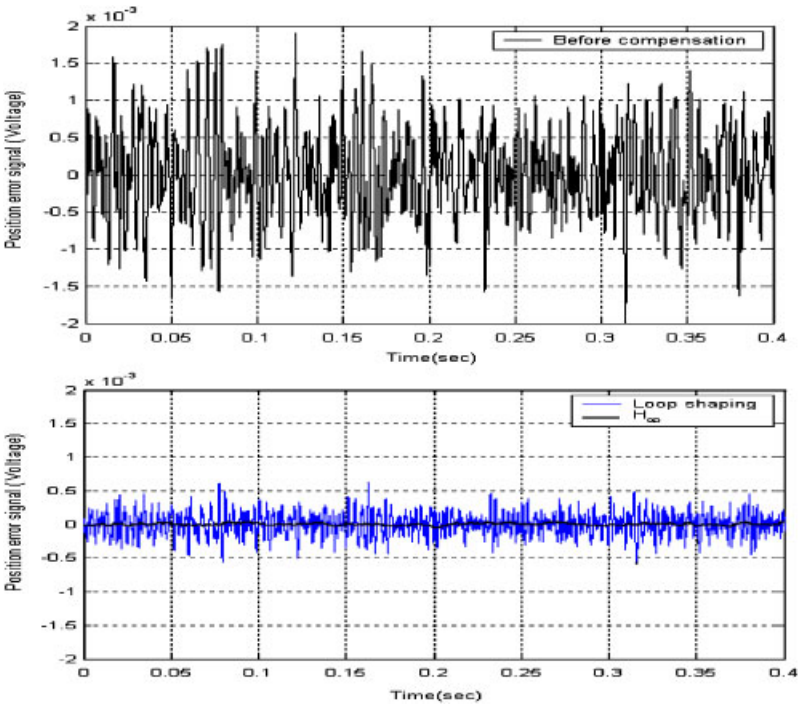

Figure 9. PES time sequence with and without the feedforward compensator (70% reduction of σ value by loop shaping method and 97% by H_∞ method).

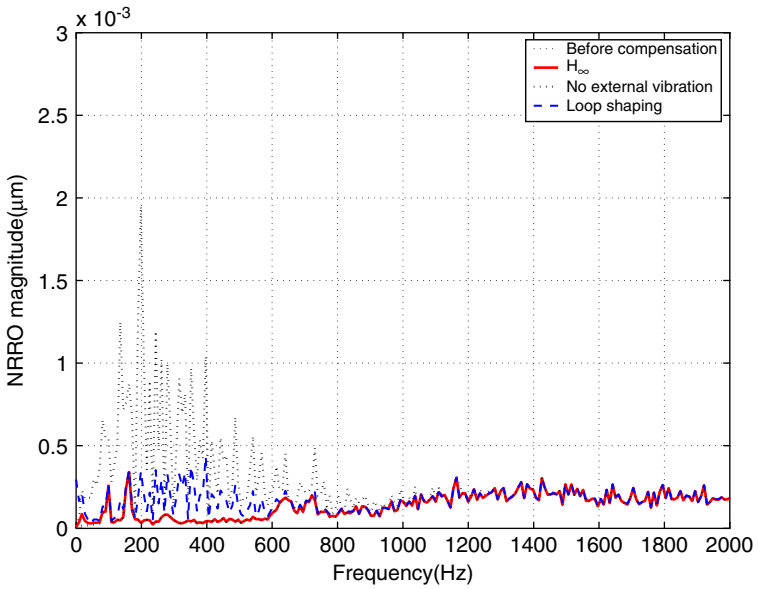

Figure 10. Position error spectrum with and without the feedforward compensation.

DOI: 10.1002/acs

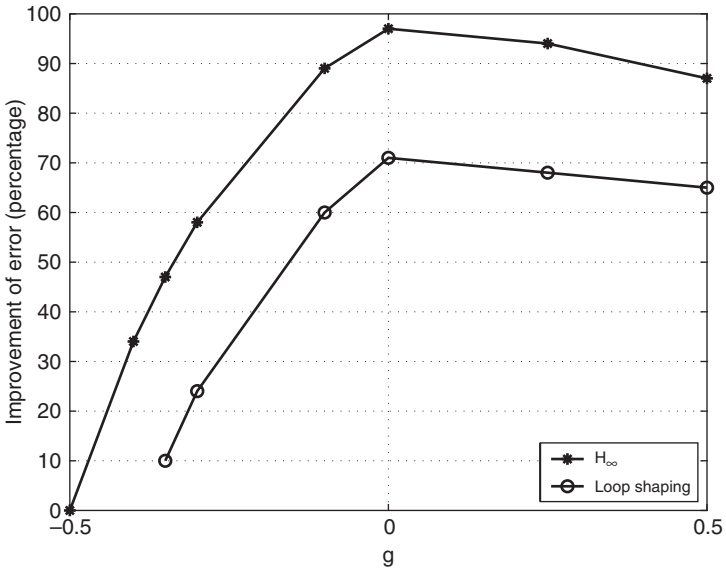

Figure 11. PES σ reduction rate *versus* g.

The compensation capability of $F(z)$ is illustrated in Figure 8, and it is observed that the magnitude of T_{ew} up to 1.6 kHz is much less with $F(z)$ in (15). The simulation of the compensation effectiveness is carried out in Matlab Simulink. In the simulation, w is represented by a white noise with $\sigma = 1$ and the sensing noise n with $\sigma = 0.01$. Figure 9 shows the error signal before and after compensation, and the σ value of the error is reduced by 70%. Its power spectrum is compared in Figure 10, where the spectrum is much lower before 800 Hz after compensation.

Suppose that the model $D(s)$ is varying by $\pm 50\%$, i.e.

$$D(s) : (1 + g)D(s) \tag{16}$$

where g is a varying scalar from -0.5 to 0.5. Figure 11 shows the improvement percentage of error signal *versus* different g. Above 30% improvement is attained with g varying in $[-0.25, 0.5]$, while there is nearly no improvement when $g < -0.35$.

4.2. H_∞ method

With the designed (A_f, B_f, C_f, D_f), the transfer function of the 17th order $F(z)$ is obtained as follows:

$$\begin{aligned} F(z) = {} & \frac{0.00019376(z-0.9941)(z-0.002893)(z+0.002676)(z^2-1.983z+0.9832)}{(z+0.9501)(z-0.9958)(z-0.9974)(z-0.9999)(z-0.9691)(z+0.1161)} \\ & \times \frac{(z^2-0.04126z+0.005365)(z^2-0.3077z+0.1866)(z^2-1.17z+0.8313)}{(z+0.1083)(z-0.0005814)(z+0.0002347)(z^2-1.968z+0.9691)} \\ & \times \frac{(z^2-1.254z+0.9652)(z^2+0.1748z+0.8138)(z^2+0.00634z+0.02087)}{(z^2-0.1034z+0.1872)(z^2-1.174z+0.8387)(z^2-1.22z+0.9646)} \end{aligned} \tag{17}$$

DOI: 10.1002/acs

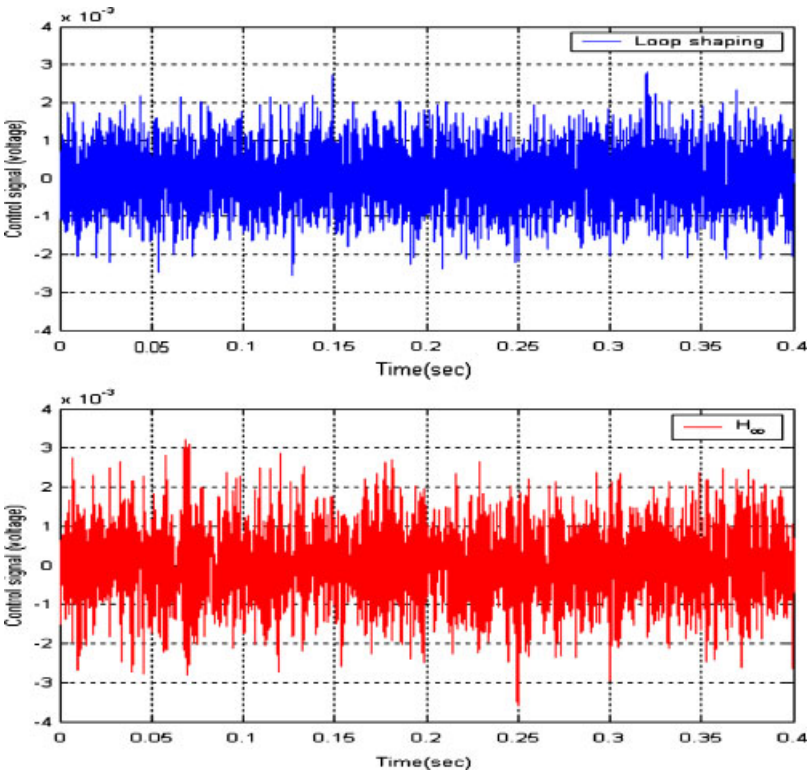

Figure 12. Control signal with loop shaping and H_∞ feedforward compensation (H_∞ method requires more control effort).

Its frequency response is drawn as solid curves in Figure 7, where apparently $F(z)$ in (17) matches $D(z)[M(z)P(z)]^{-1}$ better than $F(z)$ in (15), especially in the high-frequency range.

The comparison of T_{ew} with and without $F(z)$ is shown in Figure 8, and it is seen that the magnitude of T_{ew} is lowered further from 40 Hz up to 5 kHz, compared with the loop shaping method, although it is higher before 40 Hz. As a result, a remarkable improvement of 97% of the error signal is achieved, as seen in Figure 9. Correspondingly, the control effort is shown in Figure 12, from which we can see that the H_∞ feedforward compensation requires more control effort.

The compensation effectiveness is also reflected in Figure 10, where after compensation the effect of external vibrations is hardly seen in the spectrum of position error, and it is only slightly observed at frequencies lower than 30 Hz. Consistent with the time trace in Figure 9, it is much better than that from loop shaping method.

With $F(z)$ designed by the H_∞ method, the reduction of error signal *versus* $g = [-0.5, 0.5]$ in (16) is also evaluated and illustrated in Figure 11. It is seen that when $g = [-0.4, 0.5]$, over 30% improvement can be achieved. In this sense, it is more robust than the loop shaping method. As expected, the largest improvement occurs at $g = 0$.

Certainly, the above problem with varying $D(s)$ as described in (16) can be formulated as an uncertain H_∞ control problem, and $F(z)$ can be designed such that $\|T_{ew}\|_\infty$ is minimized in the

DOI: 10.1002/acs

Table I. Order of $F(z)$ and improvement of position error σ value.

Order of $F(z)$	17	16	14	12
Positioning accuracy improvement (%)	97	94	94	92

presence of uncertainties in the vibration model $D(s)$. Nevertheless, to deal with the problem with the consideration of variant external vibration d or together with actuator plant $P(s)$ variation, as a future work, adaptive and neural network strategies [4] will be applied for designing and adjusting the parameters of the feedforward controller $F(z)$.

To simplify $F(z)$, order reduction is conducted for (17). The orders and the achieved positioning accuracy improvements are tabulated in Table I. The transfer function of the 12th-order $F(z)$ is given in (18) with the frequency response shown as dash-dotted line in Figure 7, which is almost the same as the 17th-order $F(z)$ with only slight difference before 100 Hz. Table I indicates that with the reduced-order feedforward controller, the positioning accuracy is improved remarkablyby more than 92%

$$F(z) = \frac{0.00019376(z-0.002893)(z+0.002676)(z^2-1.983z+0.9832)(z^2-0.04126z+0.005365)}{(z+0.9501)(z-0.9691)(z-0.9974)(z-0.9999)(z+0.1161)(z+0.1083)(z-0.0005814)} \times \frac{(z^2+0.00634z+0.02087)(z^2-0.3077z+0.1866)(z^2+0.1748z+0.8138)}{(z+0.0002347)(z^2-1.968z+0.9691)(z^2-0.1034z+0.1872)} \tag{18}$$

5. CONCLUSION

In this paper, the problem of compensation for external vibration impact on positioning accuracy in disk drives has been considered. With an external vibration sensor, the feedforward scheme has been used to attenuate the impact. The loop shaping method in frequency domain and the H_∞ method in state space have been proposed to design the feedforward controller. The two methods are applied for improving the positioning accuracy of the VCM actuator in a 1.8-in small disk drive, where external vibrations are imposed vertically to the disk surface and an accelerometer is used to measure the acceleration signal due to the external vibrations. Application results have shown that the feedforward controller designed by the H_∞ method can achieve 97% reduction in error induced by external vibrations.

REFERENCES

1. Wood RW, Takano H. Prospects for magnetic recording over the next 10 years. *IEEE International Magnetics Conference 2006*, San Diego, CA, U.S.A., 8–12 May 1998.
2. Guo G, Zhang J. Control strategies for writing servo tracks narrower than 5 micro inches. *The 2003 JSME-IIP/ASME-ISPS Joint Conference on Mechatronics for Information and Precision Equipment* (*IIP/ISPS Joint MIPE'03*), Yokahama, Japan, 16–18 June 2003.
3. Ehrlich R, Adler J, Hindi H. Rejecting oscillatory, non-synchronous mechanical disturbances in hard disk drives. *IEEE Transactions on Magnetics* 2001; **37**(2):646–650.
4. Herrmann G, Ge SS, Guo G. Practical implementation of a neural network controller in a hard disk drive. *IEEE Transactions on Control Systems Technology* 2005; **13**(1):146–154.

DOI: 10.1002/acs

5. Lee HS. Controller optimization for minimum position error signals of hard disk drives. *IEEE Transactions on Industrial Electronics* 2001; **48**(5):945–950.
6. Grochowski EG, Hoyt RF, Heath JS. Magnetic hard disk drive form factor evolution. *IEEE Transactions on Magnetics* 1993; **29**(6):4065–4067.
7. Tanaka Y. Fundamental features of perpendicular magnetic recording and the design consideration for future portable HDD integration. *IEEE International Magnetics Conference*, Nagoya, Japan, 4–8 April 2005; 163–164.
8. Usui K, Kisaka M, Okuyama A, Nagashima M. Reduction of external vibration in HDDs using adaptive feedforward control with single shock sensor. *Advanced Motion Control* (*AMC*), Istanbul, Turkey, 2006; 138–142.
9. Pannu S, Horowitz R. Adaptive accelerometer feedforward servo for disk drives. *Proceedings of the 36th Conference of Decision and Control*, San Diego, CA, U.S.A., 1997; 4216–4218.
10. Bode HW. *Network Analysis and Feedback Amplifier Design*. Van Nostrand: Princeton, NJ, 1945.
11. Aruga K, Mizoshita Y, Iwatsubo M, Hatagami T. Acceleration feedforward control for head positioning in magnetic disk drives. *JSME International Journal Series III* 1990; **33**(1):35–41.
12. White MT, Tomizuka M. Increased disturbance rejection in magnetic disk drives by acceleration feedforward control and parameter adaption. *Control Engineering Practice* 1997; **5**(6):741–751.
13. Baek SE, Lee SH. Vibration rejection control for disk drives by acceleration feedforward control. *Thirty-eigth Conference of Decision and Control*, Phoenix, U.S.A., 1999.
14. Bando N, Oh S, Hori Y. External disturbance rejection control based on identification of transfer characteristics from the acceleration sensor for access control of hard disk drive system. *Advanced Motion Control* (*AMC*), Maribor, Slovenia, 2002; 52–56.
15. Guo G, Zhang J. Feedforward control for reducing disk-flutter-induced track misregistration. *IEEE Transactions on Magnetics* 2003; **39**(4):2103–2108.
16. Gahinet P, Nemirovski A, Laub AJ, Chilali M. *LMI Control Toolbox*. The Math Works Inc.: Natick, MA, 1995.
17. Du C, Guo G. Lowering the hump of sensitivity functions for discrete-time dual-stage systems. *IEEE Transactions on Control Systems Technology* 2005; **13**(5):791–798.
18. de Oliveira MC, Geromel JC, Bernussou J. An LMI optimization approach to multiobjective and robust H_∞ controller design for discrete-time systems. *Proceedings of the 38th IEEE Conference on Decision and Control*, Arizona, U.S.A., 7–10 December 1999; 3611–3616.

DOI: 10.1002/acs